This article has been accepted for publication in a future issue of this journal, but has not been fully edited. Content may change prior to final publication. Citation information: DOI 10.1109/TPWRS.2017.2776253, IEEE Transactions on Power Systems

Approximate Linear Power Flow Using Logarithmic Transform of Voltage Magnitudes with Reactive Power and Transmission Loss Consideration

Zhigang Li, *Member*, *IEEE*, Jinyu Yu, and Q. H. Wu, *Fellow*, *IEEE*

***Abstract*–Alternating current (AC) power flow (PF) presents difficulties for power system analysis and optimization due to its nonlinearity. Progress has been made to approximately linearize AC PF in recent decades. However, few studies have reported the simultaneous accurate approximation of reactive power and transmission losses. To bridge this gap, this paper investigates the linear approximation of AC PF considering the accuracy of the reactive load flows and transmission losses. Using the logarithmic transform of voltage magnitudes, a linear PF (LPF) model involving tap changers and phase shifters is derived from the approximation analysis of general branch flows. Transmission power loss and loss-concerned complex branch flow are also formulated. Cold-start and warm-start LPF calculation methods associated with injection compensation are also developed. Numerical simulations are performed to compare the proposed models and several state-of-the-art LPF models using 25 practical-scale test systems. The simulation results demonstrate the advantages of the proposed model over the other models for approximating voltage magnitudes, branch flows and power losses. The effectiveness of using proper compensation injection in improving the solution accuracy is also verified.**

***Index Terms*—DC power flow, linearization, load flow analysis, power loss, voltage, reactive power**

I. Introduction

POWER flow (PF) plays a fundamental role in various advanced applications of energy management systems, such as state estimation, optimal power flow (OPF), contingency analysis (CA), and reliability assessment [1]. Due to its nonlinearity, the analysis of alternating current (AC) PF can be computationally intensive in multistage or online applications, particularly for large-scale power systems. When involved in optimization-based applications, the inherent nonconvexity of PF could make the optimization intractable. The difficulty in handling AC PF has become one of the binding factors for power system analysis and optimization as interconnected power systems have expanded in recent years.

As an alternative to the full AC PF, linear approximation is one method for relieving the numerical burden of PF modeling and analysis. The direct-current (DC) PF has become one of the most widely used linear approximate models since it was first developed decades ago. With the assumption of flat voltage profiles and neglecting reactive power conditions, the MW flow of each branch is approximately proportional to the phase angle difference across the branch, and the resultant DC PF model is a set of linear equations that involve only the active power injections and phase angles of the bus voltages [2]. The DC PF method is simple to implement and has been extensively used or embedded in power system analysis and optimization, such as in sensitivity analyses [3], CA [4], electricity market clearing and power system scheduling [1], [5]. Although the DC PF method provides a good approximation of active load flow under certain assumptions, it may fail to yield acceptable solutions for networks with large R/X ratios [2] or with insufficiently flat voltage profiles [6]. In addition, this model is not suitable for applications where reactive branch flows or voltage magnitudes are primary concerns, such as automatic voltage control (AVC) [7].

Because the DC PF method is limited in many practical situations, efforts have recently been made to develop other types of linear PF (LPF) models. A linearized PF model that preserves the effect of reactive power is developed in [8]. Sine and cosine functions of phase angles are approximated using linear functions, by which the PF model is reformulated as linear equations of squared voltage magnitudes and-modified phase angles. The results of this model have not been reported for either voltage magnitudes or reactive branch flow. An approximate PF solution for a distribution network was analytically derived in [9]. Under certain assumptions, the voltage phasor can be approximated as a linear function of load demands at PQ buses with guaranteed error bounds. The accuracy of this approximation regarding voltage phase angles and magnitudes is verified using a modified IEEE 123-feeder test system. Reference [10] employed curve fitting to linearize the nonlinear terms of voltages in the PF model of a distribution system. The approximation errors of the active and reactive branch flows were not analyzed in [9] or [10]. An LPF model considering voltage magnitude was derived in [11]. The model in [11] includes both active and reactive power equations and assumes that the branches are lossless. The errors of the voltage magnitudes and active branch flows were small, while the results for reactive branch flows are not provided in [11]. Reference [12] developed a network model considering reactive power and transmission losses for convex relaxation in AC PF. The model is composed of two terms: one for the PF distribution that is linear to the squared voltage magnitudes and phase angles and another for the network losses that is quadratic to the same set of variables. The linear component of that model could potentially be applied in an approximate PF calculation. The quadratic network loss component was linearized in [13] using the sensitivity matrix. The resultant PF model in [13] is linear to the state variables, and it is essentially a warm-start version because a predefined base case is required to compute

This work is funded by the Fundamental Research Funds for the Central Universities (2017BQ043) and the State Key Laboratory of Control and Simulation of Power Systems and Generation Equipment (SKLD17KM07). The authors are with the School of Electric Power Engineering, South China University of Technology, Guangzhou 510641, China (e-mail: lizg16@scut.edu.cn).

This article has been accepted for publication in a future issue of this journal, but has not been fully edited. Content may change prior to final publication. Citation information: DOI 10.1109/TPWRS.2017.2776253, IEEE Transactions on Power Systems

the sensitivities. The effects of network losses are explicitly involved in the models of [12]-[13].

Progress in LPF modeling considering voltage magnitudes has been reported in recent literature; however, a limited number of studies have estimated reactive branch flows accurately. In certain security-related applications (e.g., CA and AVC), inaccurate reactive branch flows can result in misleading analysis results or even risky control decisions because both reactive and active PF contribute to the branch current. In addition, the estimation of power loss based on LPF modeling is seldom discussed in the existing related references; such estimations would be of considerable interest in economic dispatch (ED), unit commitment (UC), or cost allocation in electricity markets. To bridge these gaps, this paper presents a novel linear approximation method for the PF model. The major contributions of this paper are two-fold:

1. An approximate LPF model is derived using the logarithmic transform of voltage magnitudes (LTVM). The proposed model considers the voltage magnitudes, phase angles, and effects of active and reactive power simultaneously. The effect of network losses is also implicitly embedded in the proposed linear model. LTVM preserves part of the nonlinear effects of voltage magnitudes on both the active and reactive load flows, and the proposed model provides more accurate solutions for voltage magnitudes, branch flows and transmission power losses than the state-of-the-art LPF models. The transmission losses and active and reactive branch flows are formulated based on the LTVM. The proposed formulation of branch flows considers the transmission power loss and can be regarded as a generalization of several linear formulations of branch flows derived in the literature.

2. Two versions of the PF calculation method are developed based on the proposed linear models. As a cold-start method, the first method solves the proposed LPF directly. As a warm-start version, the second method introduces injection compensation (IC) to the LPF equations to potentially improve the solution quality given that an initial estimation of the PF solution is predefined.

The remainder of this paper is organized as follows. In Section II, the LPF models are developed, and the power loss and branch flows are formulated. In Section III, two versions of the PF methods based on the linear models are developed. In Section IV, comparative case studies are conducted to demonstrate the performance of the proposed LPF models and methods. Section V concludes this paper with discussions.

II. Approximate LPF Model

To convey the basic idea of LTVM, the LPF model without tap changers and phase shifters is derived in abstract in Section II-A. A full version of the LPF model that considers tap changers and phase shifters is developed in detail in Section II-B. The power loss and branch flow are formulated in Sections II-C and II-D, respectively.

A. Abstract of the LPF Derivation Using LTVM

The basic idea of deriving the LPF based on LTVM is introduced briefly in this subsection. The units of all variables involved are p.u. unless otherwise noted. Symbols in bold denote matrices or vectors. The well-known AC PF in polar form can be expressed as follows:

$$\begin{cases} P_i = \mathrm{Re}\left(V_i \sum_j V_j e^{\mathrm{j}\theta_{ij}} (G_{ij} - \mathrm{j}B_{ij})\right) \\ Q_i = \mathrm{Im}\left(V_i \sum_j V_j e^{\mathrm{j}\theta_{ij}} (G_{ij} - \mathrm{j}B_{ij})\right) \end{cases} \Leftrightarrow \begin{cases} P_i e^{-\ln V_i} = \mathrm{Re}\left(\sum_j e^{\ln V_j + \mathrm{j}\theta_{ij}} (G_{ij} - \mathrm{j}B_{ij})\right) \\ Q_i e^{-2\ln V_i} = \mathrm{Im}\left(\sum_j e^{\ln V_j - \ln V_i + \mathrm{j}\theta_{ij}} (G_{ij} - \mathrm{j}B_{ij})\right) \end{cases}, \tag{1}$$

where P_i and Q_i denote the net power injection of active and reactive power at bus i, respectively; G_{ij} and B_{ij} denote the real and imaginary part of nodal admittance Y_{ij}, respectively; V_i denotes the voltage magnitude of bus i; θ_{ij} denotes the voltage phase angle difference between buses i and j.

To focus on the basic idea of LPF derivation, we do not consider the effects of tap changers and phase shifters temporarily. For normally operating power systems, we have $\theta_{ij} \approx 0$ rad, $V_i \approx V_j \approx 1$ p.u. The *modified voltage magnitude*, symbolized as u_i, is defined as a logarithmic transform of the original voltage magnitude from the V-space into the u-space:

$$u_i = \ln V_i, u_{ij} = u_i - u_j = \ln V_i - \ln V_j, \tag{2}$$

where u_{ij} is called the *modified voltage magnitude difference*. Obviously, $V_i \approx V_j \approx 1$ implies $u_i \approx 0$ and $u_{ij} \approx 0$; therefore,

$$\begin{aligned} &e^{-u_i} \approx 1 - u_i, e^{u_j + \mathrm{j}\theta_{ij}} \approx 1 + u_j + \mathrm{j}\theta_{ij}, \\ &e^{-2u_i} \approx 1 - 2u_i, e^{-u_{ij} + \mathrm{j}\theta_{ij}} \approx 1 - u_{ij} + \mathrm{j}\theta_{ij} \end{aligned}. \tag{3}$$

Employing the LTVM and substituting (3) into (1) yields:

$$\begin{cases} P_i(1 - u_i) \approx \sum_j \left[G_{ij}(1 + u_j) + B_{ij}\theta_{ij} \right] \\ Q_i(1 - 2u_i) \approx \sum_j \left[-B_{ij}(1 - u_{ij}) + G_{ij}\theta_{ij} \right] \end{cases}. \tag{4}$$

After a simple manipulation of (4), we obtain the following:

$$\begin{aligned} P_i - \sum_j G_{ij} \approx &\left(P_i + G_{ii}\right)u_i + \sum_{j \neq i} G_{ij} u_j \\ &+ \left(\sum_{j \neq i} B_{ij}\right)\theta_i - \sum_{j \neq i} B_{ij}\theta_j \end{aligned}, \tag{5}$$

$$\begin{aligned} Q_i + \sum_j B_{ij} \approx &\left(2Q_i + \sum_{j \neq i} B_{ij}\right)u_i - \sum_{j \neq i} B_{ij} u_j \\ &+ \left(\sum_{j \neq i} G_{ij}\right)\theta_i - \sum_{j \neq i} G_{ij}\theta_j \end{aligned}, \tag{6}$$

where θ_i denotes the voltage phase angle of bus i.

As boundary conditions for the AC PF computation, the nodal net power injections of the PQ buses and the nodal net active power injections of the PV buses are predefined. Therefore, the approximate nodal power equations of the PQ and PV buses presented in (5) and (6) are linear to the transformed state variables. Equations (5) and (6) constitute an LPF model for the approximate PF computation.

Discussions: 1. Preserved nonlinearity. Although the equations in (5) and (6) are linear to $\boldsymbol{u}$ and $\boldsymbol{\theta}$, the nonlinearity of the PF equations are still preserved. Starting from (4), we obtain

$$\begin{cases} P_i \approx \sum_j \left[G_{ij}(1 + \ln V_j) + B_{ij}\theta_{ij} \right] \Big/ (1 - \ln V_i) \\ Q_i \approx \sum_j \left[-B_{ij}(1 - \ln V_i + \ln V_j) + G_{ij}\theta_{ij} \right] \Big/ (1 - 2\ln V_i) \end{cases}. \tag{7}$$

Obviously, $\boldsymbol{V}$ and $\boldsymbol{\theta}$ still hold a nonlinear relationship in (7), although (5) and (6) are linear equations. Due to the preserved nonlinearity, the effects of the voltage magnitudes and phase angles on the active and reactive load flows as well as the power losses are reflected approximately in (5) and (6). This feature enables the proposed model to provide good approximations of the PFs.

This article has been accepted for publication in a future issue of this journal, but has not been fully edited. Content may change prior to final publication. Citation information: DOI 10.1109/TPWRS.2017.2776253, IEEE Transactions on Power Systems

2. The effect of nonlinear transformation. The LTVM is applied in the proposed model to transform the coordinates of state variables, with which the LPF model is derived. Indeed, other types of nonlinear transformation of state variables have been performed to derive different LPF models in the literature [8],[12]. As numerically demonstrated in Section IV-D, LTVM can be used to approximate the nonlinear terms in AC PF more accurately than other state-of-the-art methods. In addition, the nonlinear terms in P and Q equations are handled in different ways, although both are based on LTVM, by exploiting the physical features of practical power networks. This scheme provides accurate approximations of both P and Q equations, In addition, it preserves the linearizability of the proposed LPF model. Detailed analysis of the effect of using the proposed nonlinear transformation technique is referred in Section IV-D.

3. Comparison with [14]. In our paper, the log-voltage magnitudes are defined in place of the original voltage magnitudes to derive the linear approximation of PF, and the resultant LPF model is described in the $(\boldsymbol{u},\boldsymbol{\theta})$ space. LTVM is also involved in the recent work of [14], where it is employed to define the objective function or energy function instead of performing linearization. In [14], the original voltage magnitudes are not replaced with their logarithmic values, and the AC PF model is still formulated in the $(\boldsymbol{v},\boldsymbol{\theta})$ space.

The derivation of the LPF model in this subsection does not consider tap changers and phase shifters for simplicity. The involvement of these elements would cause nontrivial changes in the coefficients in (5) and (6) and requires a thorough analysis regarding the branch flows. Based on the concept of LTVM, a full version of the LPF model with tap changers and phase shifters will be derived in detail in the next subsection.

B. Detailed Derivation of LPF with General Branches

An approximation analysis of the general branch model is performed before the development of the full LPF model.

1) Approximate Analysis of a General Branch

The branch model shown in Fig. 1 consists of a π-type line and an ideal phase-shifting transformer, and this model is general enough to describe the transmission lines, transformers and phase shifters [15]. The branch model is directed with buses *i* and *j*, which are denoted as the *from-end* and *to-end buses*, respectively. The currents in this branch are approximately analyzed in the following diagram.

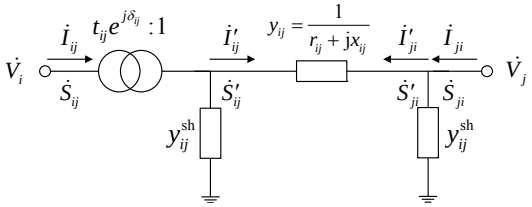

Fig. 1. General branch with a tap changer and a phase shifter.

The branch currents in both directions are as follows:

$$\dot{I}_{ij}=\frac{y_{ij}^{\mathrm{sh}}+y_{ij}}{t_{ij}^2}\dot{V}_i-\frac{y_{ij}}{t_{ij}e^{-\mathrm{j}\delta_{ij}}}\dot{V}_j\,, \tag{8}$$

$$\dot{I}_{ji}=-\frac{y_{ij}}{t_{ij}e^{\mathrm{j}\delta_{ij}}}\dot{V}_i+(y_{ij}^{\mathrm{sh}}+y_{ij})\dot{V}_j\,, \tag{9}$$

where $\dot{I}_{ij}$ denotes the branch current from bus *i* to bus *j*; y_{ij}^{sh}, y_{ij}, t_{ij}, and δ_{ij} denote the shunt admittance, serial admittance, tap ratio, and phase shift angle of the general branch (i,j), respectively.

The voltage phasors $\dot{V}_i$ in (8) are replaced with its exponential form $\dot{V}_i=V_ie^{\mathrm{j}\theta_i}$, which yields

$$\begin{aligned}\dot{I}_{ij}e^{-\mathrm{j}\theta_i}&=\frac{y_{ij}^{\mathrm{sh}}}{t_{ij}}\cdot\frac{V_i}{t_{ij}}+\frac{y_{ij}}{t_{ij}}\left(\frac{V_i}{t_{ij}}-V_je^{-\mathrm{j}(\theta_{ij}-\delta_{ij})}\right)\\&=\frac{y_{ij}^{\mathrm{sh}}}{t_{ij}}e^{\ln(V_i/t_{ij})}+\frac{y_{ij}}{t_{ij}}\left[e^{\ln(V_i/t_{ij})}-e^{\ln V_j-\mathrm{j}(\theta_{ij}-\delta_{ij})}\right]\end{aligned}\,. \tag{10}$$

In normal operation conditions for practical power systems, it is reasonable to assume that $V_i\approx 1$, $V_i/t_{ij}\approx 1$, and $\theta_{ij}-\delta_{ij}\approx 0$ [16]. The first-order expansion is applied to the exponentials in (10) to yield the following phase-shifted from-end current

$$\dot{I}_{ij}e^{-\mathrm{j}\theta_i}\approx\frac{y_{ij}^{\mathrm{sh}}}{t_{ij}}\left(1+u_i-t'_{ij}\right)+\frac{y_{ij}}{t_{ij}}\left[u_{ij}-t'_{ij}+\mathrm{j}(\theta_{ij}-\delta_{ij})\right], \tag{11}$$

where $u_i=\ln V_i$, $u_{ij}=u_i-u_j$, and $t_{ij}'=\ln t_{ij}$. The phase-shifted to-end current in (9) can be similarly approximated by

$$\dot{I}_{ji}e^{-\mathrm{j}\theta_j}\approx y_{ij}\left[u_{ji}+t'_{ij}+\mathrm{j}(\theta_{ji}+\delta_{ij})\right]+y_{ij}^{\mathrm{sh}}(1+u_j)\,. \tag{12}$$

Dividing both sides of (8) by $\dot{V}_i$ yields

$$\begin{aligned}\frac{\dot{I}_{ij}}{\dot{V}_i}&=\frac{y_{ij}^{\mathrm{sh}}+y_{ij}}{t_{ij}^2}-\frac{y_{ij}}{t_{ij}^2}\cdot\frac{t_{ij}V_j}{V_i}e^{-\mathrm{j}(\theta_{ij}-\delta_{ij})}\\&\approx\frac{y_{ij}^{\mathrm{sh}}+y_{ij}}{t_{ij}^2}-\frac{y_{ij}}{t_{ij}^2}e^{\ln(t_{ij}V_j/V_i)-\mathrm{j}(\theta_{ij}-\delta_{ij})}\\&\approx\frac{y_{ij}^{\mathrm{sh}}}{t_{ij}^2}+\frac{y_{ij}}{t_{ij}^2}\left[u_{ij}-t'_{ij}+\mathrm{j}(\theta_{ij}-\delta_{ij})\right]\end{aligned}\,, \tag{13}$$

where the approximation holds because the voltage magnitude difference across a transmission line is typically small, i.e., $V_i/t_{ij}\approx V_j$. Similarly, (9) can be simplified to the following:

$$\frac{\dot{I}_{ji}}{\dot{V}_j}\approx y_{ij}^{\mathrm{sh}}+y_{ij}\left[u_{ji}+t'_{ij}+\mathrm{j}(\theta_{ji}+\delta_{ij})\right]. \tag{14}$$

Equations (11)-(14), which are linear to the modified voltage magnitudes and phase angles, will be utilized in the following derivation of the approximate LPF model.

2) Derivation of the Approximate LPF Model

(a) Nodal Active Power Equations

The nodal complex power injection is as follows:

$$\dot{S}_i=\dot{V}_i\dot{I}_i^*=V_ie^{\mathrm{j}\theta_i}\cdot\dot{I}_i^*\;\Rightarrow\;\dot{S}_i^*V_i^{-1}=\dot{I}_ie^{-\mathrm{j}\theta_i}\,, \tag{15}$$

where $\dot{S}_i$ and $\dot{I}_i$ denote the net injection of complex power and current at bus *i*, respectively.

According to Kirchhoff's current law (KCL), the net current injection at each bus *i* is subject to the following:

$$\dot{I}_i=\dot{I}_{i0}+\sum\nolimits_{j\in\mathrm{TE}(i)}\dot{I}_{ij}+\sum\nolimits_{i\in\mathrm{TE}(k)}\dot{I}_{ik}\,, \tag{16}$$

where the three terms on the right denote the current through the shunt branch at bus *i*, the summed currents of the branches with from-end buses *i*, and those with to-end buses *i*, respectively; TE(*i*) denotes the index set of the to-end buses of the directed branches with from-end bus *i*. Because $V_i\approx 1$, we obtain the following:

This article has been accepted for publication in a future issue of this journal, but has not been fully edited. Content may change prior to final publication. Citation information: DOI 10.1109/TPWRS.2017.2776253, IEEE Transactions on Power Systems

$$\dot{S}_i^* V_i^{-1} = \dot{S}_i^* e^{-\ln V_i} \approx \dot{S}_i^* (1-u_i). \quad (17)$$

Substituting (11)-(12) and (16)-(17) into (15) yields

$$\dot{S}_i'^* = y_i^{\mathrm{sh}\prime} u_i + \sum\nolimits_j y'_{ij}(u_{ij} + \mathrm{j}\theta_{ij}), \quad (18)$$

where

$$\dot{S}_i'^* = \dot{S}_i^* - \sum_{j\in \mathrm{TE}(i)} \left[y_{ij}^{\mathrm{sh}}(1-t'_{ij}) - y_{ij}(t'_{ij} + \mathrm{j}\delta_{ij}) \right] / t_{ij} - \sum_{i\in \mathrm{TE}(k)} \left[y_{ki}^{\mathrm{sh}} + y_{ki}(t'_{ki} + \mathrm{j}\delta_{ki}) \right] - y_{i0}, \quad (19)$$

$$y_i^{\mathrm{sh}\prime} = \dot{S}_i^* + y_{i0} + \sum_{j\in \mathrm{TE}(i)} y_{ij}^{\mathrm{sh}} / t_{ij} + \sum_{i\in \mathrm{TE}(k)} y_{ki}^{\mathrm{sh}}, \quad (20)$$

$$y'_{ij} = \begin{cases} y_{ij}/t_{ij}, & \text{if } j \in \mathrm{TE}(i) \\ y_{ji}, & \text{if } i \in \mathrm{TE}(j) \\ 0, & \text{otherwise} \end{cases}. \quad (21)$$

In (20), y_{i0} denotes the shunt admittance at bus i. Let $\dot{S}'_i = P'_i + \mathrm{j}Q'_i$, $y_i^{\mathrm{sh}\prime} = g_i^{\mathrm{sh}\prime} + \mathrm{j}b_i^{\mathrm{sh}\prime}$, and $y'_{ij} = g'_{ij} + \mathrm{j}b'_{ij}$. Taking the real part of both sides in (18) yields

$$P'_i = \tilde{G}'_{ii} u_i + \sum\nolimits_{j\neq i} G'_{ij} u_j - \sum\nolimits_j B'_{ij} \theta_j, \quad (22)$$

where

$$G'_{ij} = -g'_{ij} \ (j \neq i), \ \tilde{G}'_{ii} = g_i^{\mathrm{sh}\prime} + \sum\nolimits_{j\neq i} g'_{ij}, \quad (23)$$

$$B'_{ij} = -b'_{ij} \ (j \neq i), \ B'_{ii} = \sum\nolimits_{j\neq i} b'_{ij}. \quad (24)$$

Equation (22) is the active power equation of the proposed LPF model, where the modified active power injection is linear to the modified voltage magnitudes and phase angles.

(b) Nodal Reactive Power Equations

By starting from (15) and combining (16), we obtain

$$\dot{S}_i^* V_i^{-2} = \dot{I}_i \dot{V}_i^{-1} = y_{i0} + \sum\nolimits_{j\in \mathrm{TE}(i)} \dot{I}_{ij} \dot{V}_i^{-1} + \sum\nolimits_{i\in \mathrm{TE}(k)} \dot{I}_{ik} \dot{V}_i^{-1}. \quad (25)$$

The assumption that $V_i \approx 1$ yields

$$\dot{S}_i^* V_i^{-2} = \dot{S}_i^* e^{-2\ln V_i} \approx \dot{S}_i^* (1-2u_i). \quad (26)$$

Combining (13), (14), (25) and (26), we obtain

$$\dot{S}_i''^* = 2\dot{S}_i^* \cdot u_i + \sum\nolimits_j y''_{ij}(u_{ij} + \mathrm{j}\theta_{ij}), \quad (27)$$

where

$$\dot{S}_i''^* = \dot{S}_i^* - \sum_{j\in \mathrm{TE}(i)} \left[y_{ij}^{\mathrm{sh}} - y_{ij}(t'_{ij} + \mathrm{j}\delta_{ij}) \right] / t_{ij}^2 - \sum_{i\in \mathrm{TE}(k)} \left[y_{ki}^{\mathrm{sh}} + y_{ki}(t'_{ki} + \mathrm{j}\delta_{ki}) \right] - y_{i0}, \quad (28)$$

$$y''_{ij} = \begin{cases} y_{ij}/t_{ij}^2, & \text{if } j \in \mathrm{TE}(i) \\ y_{ji}, & \text{if } i \in \mathrm{TE}(j) \\ 0, & \text{otherwise} \end{cases}. \quad (29)$$

Let $\dot{S}''_i = P''_i + \mathrm{j}Q''_i$ and $y''_{ij} = g''_{ij} + \mathrm{j}b''_{ij}$. Taking the imaginary part of both sides in (27) yields

$$Q''_i = -\tilde{B}''_{ii} u_i - \sum\nolimits_{j\neq i} B''_{ij} u_j - \sum\nolimits_j G''_{ij} \theta_j, \quad (30)$$

where

$$B''_{ij} = -b''_{ij} \ (j \neq i), \ \tilde{B}''_{ii} = -2Q_i + \sum\nolimits_{j\neq i} b''_{ij}, \quad (31)$$

$$G''_{ij} = -g''_{ij} \ (j \neq i), \ G''_{ii} = \sum\nolimits_{j\neq i} g''_{ij}. \quad (32)$$

Equation (30) is the reactive power equation of the proposed LPF model. The proposed LPF model considering tap changers and phase shifters is described by (22) and (30) together.

C. Formulation of the Power Loss in the Branches

1) Power Loss in a Series Branch

The current $\dot{I}'_{ij}$ through the series branch in Fig. 1 is expressed as follows:

$$\dot{I}'_{ij} = \left(\frac{\dot{V}_i}{t_{ij} e^{\mathrm{j}\delta_{ij}}} - \dot{V}_j \right) y_{ij} = \left[\frac{V_i}{t_{ij}} - V_j e^{-j(\theta_{ij}-\delta_{ij})} \right] \frac{y_{ij}}{e^{\mathrm{j}(\delta_{ij}-\theta_i)}} \approx \left[u_{ij} - t'_{ij} + \mathrm{j}(\theta_{ij} - \delta_{ij}) \right] \cdot \frac{y_{ij}}{e^{\mathrm{j}(\delta_{ij}-\theta_i)}}. \quad (33)$$

The complex power loss in the series branch $\dot{s}_{ij}^{\mathrm{loss}}$ is formulated as follows:

$$\dot{s}_{ij}^{\mathrm{loss}} = \left\| \dot{I}'_{ij} \right\|^2 \cdot (r_{ij} + \mathrm{j}x_{ij}) \approx \left\| u_{ij} - t'_{ij} + \mathrm{j}(\theta_{ij} - \delta_{ij}) \right\|^2 \cdot \left\| y_{ij} \right\|^2 \cdot (r_{ij} + \mathrm{j}x_{ij}), = \left[(u_{ij} - t'_{ij})^2 + (\theta_{ij} - \delta_{ij})^2 \right] \cdot y_{ij}^* \quad (34)$$

from which the active and reactive power losses are obtained:

$$p_{ij}^{\mathrm{loss}} = g_{ij} \cdot \left[(u_{ij} - t'_{ij})^2 + (\theta_{ij} - \delta_{ij})^2 \right], \quad (35)$$

$$q_{ij}^{\mathrm{loss}} = -b_{ij} \cdot \left[(u_{ij} - t'_{ij})^2 + (\theta_{ij} - \delta_{ij})^2 \right] \quad (36)$$

where r_{ij}, x_{ij}, g_{ij}, and b_{ij} denote the resistance, reactance, conductance, and susceptance of the general branch (i,j), respectively.

2) Power Loss in a Shunt Branch

The complex, active and reactive power losses in the aggregated shunt admittance are calculated as follows:

$$\dot{s}_i^{\mathrm{lsh}} = V_i^2 \cdot y_i^{\mathrm{sh}*} \approx (1+u_i)^2 \cdot y_i^{\mathrm{sh}*}, \quad (37)$$

$$p_i^{\mathrm{lsh}} \approx g_i^{\mathrm{sh}} \cdot (1+u_i)^2, \ q_i^{\mathrm{lsh}} \approx -b_i^{\mathrm{sh}} \cdot (1+u_i)^2, \quad (38)$$

where y_i^{sh}, b_i^{sh} and g_i^{sh} denote the total shunt admittance, conductance, and susceptance at bus i, respectively.

D. Formulation of Branch Flow with Power Loss

The branch flows at both ends of the series branch in Fig. 1 are subject to the KCL:

$$\dot{I}'_{ij} + \dot{I}'_{ji} = \left(\frac{\dot{S}'_{ij}}{\dot{V}_i / t_{ij} e^{\mathrm{j}\delta_{ij}}} \right)^* + \left(\frac{\dot{S}'_{ji}}{\dot{V}_j} \right)^* = 0. \quad (39)$$

The branch flows at both ends are also subject to the law of energy conservation:

$$\dot{S}'_{ij} + \dot{S}'_{ji} = \dot{s}_{ij}^{\mathrm{loss}}. \quad (40)$$

Combining (39) and (40), we can solve for the branch flows:

$$\dot{S}'_{ij} = -\frac{\dot{K}_{ij}}{\dot{K}_{ij}^{-1} - \dot{K}_{ij}} \dot{s}_{ij}^{\mathrm{loss}}, \ \dot{S}'_{ji} = \frac{\dot{K}_{ij}^{-1}}{\dot{K}_{ij}^{-1} - \dot{K}_{ij}} \dot{s}_{ij}^{\mathrm{loss}}, \quad (41)$$

where

$$\dot{K}_{ij} = \left[\frac{V_i}{t_{ij} V_j} e^{\mathrm{j}(\theta_{ij}-\delta_{ij})} \right]^{1/2} \approx 1 + \frac{1}{2} \left[u_{ij} - t'_{ij} + \mathrm{j}(\theta_{ij} - \delta_{ij}) \right], \quad (42)$$

$$\dot{K}_{ij}^{-1} = \left[\frac{V_i}{t_{ij} V_j} e^{\mathrm{j}(\theta_{ij}-\delta_{ij})} \right]^{-1/2} \approx 1 - \frac{1}{2} \left[u_{ij} - t'_{ij} + \mathrm{j}(\theta_{ij} - \delta_{ij}) \right]. \quad (43)$$

Substituting (34) and (42)-(43) into (41) yields

This article has been accepted for publication in a future issue of this journal, but has not been fully edited. Content may change prior to final publication. Citation information: DOI 10.1109/TPWRS.2017.2776253, IEEE Transactions on Power Systems

$$\dot{S}'_{ij} \approx y^*_{ij}\left[1+\frac{1}{2}(u_{ij}-t'_{ij})+\frac{\mathrm{j}}{2}(\theta_{ij}-\delta_{ij})\right]\cdot\left[u_{ij}-t'_{ij}-\mathrm{j}(\theta_{ij}-\delta_{ij})\right], \quad (44)$$

$$\dot{S}'_{ji} \approx -y^*_{ij}\left[1-\frac{1}{2}(u_{ij}-t'_{ij})-\frac{\mathrm{j}}{2}(\theta_{ij}-\delta_{ij})\right]\cdot\left[u_{ij}-t'_{ij}-\mathrm{j}(\theta_{ij}-\delta_{ij})\right]. \quad (45)$$

Equations (44) and (45) represent the complex branch flow with power loss. By taking the real and imaginary parts, we can obtain the following expressions:

$$P'_{ij} = p'_{ij} + 0.5\,p^{\text{loss}}_{ij}\ ,\ P'_{ji} = p'_{ji} + 0.5\,p^{\text{loss}}_{ij}\ , \quad (46)$$

$$Q'_{ij} = q'_{ij} + 0.5q^{\text{loss}}_{ij}\ ,\ Q'_{ji} = q'_{ji} + 0.5q^{\text{loss}}_{ij}\ , \quad (47)$$

where

$$p'_{ij} = -p'_{ji} = g_{ij}(u_{ij}-t'_{ij}) - b_{ij}(\theta_{ij}-\delta_{ij})\ , \quad (48)$$

$$q'_{ij} = -q'_{ji} = -b_{ij}(u_{ij}-t'_{ij}) - g_{ij}(\theta_{ij}-\delta_{ij})\ . \quad (49)$$

Equations (46) and (47) denote the active and reactive branch flows with power losses, respectively. In either equation, the first term on the right of the equality denotes the lossless component, and the second term accounts for the branch power loss.

Discussions: The branch flow formulation can be further simplified with additional assumptions. For example, if branches are assumed lossless, the second term in (46) can be omitted. Thus, the active branch flow becomes equal to its lossless component:

$$P'_{ij} = -P'_{ji} \approx p'_{ij} = g_{ij}(u_{ij}-t'_{ij}) - b_{ij}(\theta_{ij}-\delta_{ij})\ , \quad (50)$$

which is similar to the lossless MW flow derived in [11].

If the assumptions of DC PF are made, i.e., g_{ij}=0, b_{ij}=–1/x_{ij}, u_i=0, and t_{ij}'=0, the active branch flow reduces to

$$P'_{ij} = -P'_{ji} \approx (\theta_{ij}-\delta_{ij})/x_{ij}\ , \quad (51)$$

which is the branch flow formulation in the DC PF model [2]. The proposed branch flow formulation is indeed a general version that can be fitted into various situations in the literature with additional assumptions and boundary conditions.

III. LPF Methods With the Linearized Model

Two methods for the approximate LPF calculation are developed. Section III-A presents the cold-start version that involves the proposed LPF models without IC. Section III-B describes the warm-start method that incorporates the proposed LPF models with IC to further improve the solution quality.

A. Approximate LPF Without IC

Let the phase angles of the PQ, PV, and Vθ buses be $\boldsymbol{\theta}_{\text{PQ}}$, $\boldsymbol{\theta}_{\text{PV}}$, and $\theta_{\text{V}\theta}$, respectively, and the corresponding modified voltage magnitudes of the three types of buses be $\boldsymbol{u}_{\text{PQ}}$, $\boldsymbol{u}_{\text{PV}}$, and $u_{\text{V}\theta}$, respectively. Based on the LPF model derived in Section II, the PF equations for the PQ and PV buses can be stylized in a matrix form:

$$\begin{bmatrix}\tilde{\boldsymbol{P}}'_{\text{PQ}}\\ \tilde{\boldsymbol{P}}'_{\text{PV}}\\ \tilde{\boldsymbol{Q}}''_{\text{PQ}}\end{bmatrix} = -\begin{bmatrix}\boldsymbol{B}'_{\text{PQ,PQ}} & \boldsymbol{B}'_{\text{PQ,PV}} & -\tilde{\boldsymbol{G}}'_{\text{PQ,PQ}}\\ \boldsymbol{B}'_{\text{PV,PQ}} & \boldsymbol{B}'_{\text{PV,PV}} & -\tilde{\boldsymbol{G}}'_{\text{PV,PQ}}\\ \boldsymbol{G}''_{\text{PQ,PQ}} & \boldsymbol{G}''_{\text{PQ,PV}} & \tilde{\boldsymbol{B}}''_{\text{PQ,PQ}}\end{bmatrix}\begin{bmatrix}\boldsymbol{\theta}_{\text{PQ}}\\ \boldsymbol{\theta}_{\text{PV}}\\ \boldsymbol{u}_{\text{PQ}}\end{bmatrix}, \quad (52)$$

where $[\tilde{\boldsymbol{P}}'^{T}_{\text{PQ}}, \tilde{\boldsymbol{P}}'^{T}_{\text{PV}}, \tilde{\boldsymbol{Q}}''^{T}_{\text{PQ}}]^T$ are calculated using the predefined conditions of a PF problem as follows:

$$\begin{bmatrix}\tilde{\boldsymbol{P}}'_{\text{PQ}}\\ \tilde{\boldsymbol{P}}'_{\text{PV}}\\ \tilde{\boldsymbol{Q}}''_{\text{PQ}}\end{bmatrix} = \begin{bmatrix}\boldsymbol{P}'_{\text{PQ}}\\ \boldsymbol{P}'_{\text{PV}}\\ \boldsymbol{Q}''_{\text{PQ}}\end{bmatrix} + \begin{bmatrix}\boldsymbol{B}'_{\text{PQ,V}\theta} & -\tilde{\boldsymbol{G}}'_{\text{PQ,PV}} & -\tilde{\boldsymbol{G}}'_{\text{PQ,V}\theta}\\ \boldsymbol{B}'_{\text{PV,V}\theta} & -\tilde{\boldsymbol{G}}_{\text{PV,PV}} & -\tilde{\boldsymbol{G}}'_{\text{PV,V}\theta}\\ \boldsymbol{G}''_{\text{PQ,V}\theta} & \tilde{\boldsymbol{B}}''_{\text{PQ,PV}} & \tilde{\boldsymbol{B}}''_{\text{PQ,V}\theta}\end{bmatrix}\begin{bmatrix}\theta_{\text{V}\theta}\\ \boldsymbol{u}_{\text{PV}}\\ u_{\text{V}\theta}\end{bmatrix}. \quad (53)$$

All symbols in (52), except the unknown state variables $[\boldsymbol{\theta}^T_{\text{PQ}}, \boldsymbol{\theta}^T_{\text{PV}}, \boldsymbol{u}^T_{\text{PQ}}]^T$, are constants determined by network parameters and other known operation conditions. Hence, (52) is a set of LPF equations that yields an approximate solution of unknown variables to the original AC PF. This set of linear equations can be solved in one shot without any iterations. After solving (52), the phase angles of the PQ and PV buses (i.e., $\boldsymbol{\theta}_{\text{PQ}}$, $\boldsymbol{\theta}_{\text{PV}}$) are obtained directly, and the voltage magnitudes of the PQ buses can be recovered by taking the exponential of $\boldsymbol{u}_{\text{PQ}}$. Then, the load flows and power losses of the branches can be computed using the formulations in Sections II-C and II-D.

The LPF equation in (52) is free of any predefined operation points in the power system; hence, the LPF equation is a cold-start version of the LPF model [2]. Equation (52) is called the *linear approximate PF without IC* (LPF-NIC).

B. Approximate LPF With IC

The LPF equations in (53) are rewritten in an abstract form:

$$\boldsymbol{A}\boldsymbol{x} = \boldsymbol{d}\ , \quad (54)$$

where $\boldsymbol{x}$ denotes the unknown variables and $\boldsymbol{A}$ and $\boldsymbol{d}$ are the constant coefficients. The full version of the nonlinear AC PF equations in polar form is also expressed in an abstract form:

$$\boldsymbol{F}(\boldsymbol{x}) = 0\ . \quad (55)$$

Assume that $\boldsymbol{x}^*$ is a solution to the AC PF equations, i.e., $\boldsymbol{F}(\boldsymbol{x}^*)=\boldsymbol{0}$. It can be verified that $\boldsymbol{x}^*$ also satisfies the following:

$$\boldsymbol{A}\boldsymbol{x}^* = \boldsymbol{d} + [\boldsymbol{A}\boldsymbol{x}^* - \boldsymbol{d} - \boldsymbol{F}(\boldsymbol{x}^*)] = \boldsymbol{d} + \Delta\boldsymbol{d}(\boldsymbol{x}^*)\ . \quad (56)$$

Equation (56) demonstrates that the AC PF solution $\boldsymbol{x}^*$ does not satisfy the LPF model in (54) unless $\Delta\boldsymbol{d}(\boldsymbol{x}^*)$ is added to the right-hand vector. Physically, $\boldsymbol{d}$ denotes the modified nodal power injections in the LPF model. In addition, $\Delta\boldsymbol{d}(\boldsymbol{x}^*)$, which is called the IC, can be viewed as the gap in the nodal power injections between the linearized and the original nonlinear models. Solving the following equation yields an accurate solution to the AC PF:

$$\boldsymbol{A}\boldsymbol{x} = \boldsymbol{d} + \Delta\boldsymbol{d}(\boldsymbol{x}^*)\ . \quad (57)$$

The introduction of $\Delta\boldsymbol{d}(\boldsymbol{x}^*)$ helps improve the solution quality of the LPF model. However, knowing $\boldsymbol{x}^*$ beforehand is seldom realistic. Alternatively, an approximate solution of $\boldsymbol{x}^{(0)}$ to the AC PF is accessible. Given that $\boldsymbol{x}^{(0)}$ is close to the accurate solution, it could still be used to approximate the IC $\Delta\boldsymbol{d}(\boldsymbol{x}^*)$, and the following linear equation is formulated:

$$\boldsymbol{A}\boldsymbol{x} = \boldsymbol{d} + \Delta\boldsymbol{d}(\boldsymbol{x}^{(0)})\ , \quad (58)$$

which is called the *approximate LPF with IC* (LPF-IC).

Here, $\boldsymbol{x}^{(0)}$ is used to induce the IC and is called the *compensation point*, and $\boldsymbol{x}^{(0)}$ can be base case operating points of the power system or obtained by any available LPF technique. The selection of $\boldsymbol{x}^{(0)}$ affects the quality of the solution to (58), and this effect depends on the similarity between $\boldsymbol{x}^{(0)}$ and $\boldsymbol{x}^*$. Because a priori knowledge of the compensation point is required, the LPF-IC is a warm-start linearization technique.

IV. Case Study

Case studies were performed to demonstrate the performance of the proposed LPF model. The first test, which is pre-

This article has been accepted for publication in a future issue of this journal, but has not been fully edited. Content may change prior to final publication. Citation information: DOI 10.1109/TPWRS.2017.2776253, IEEE Transactions on Power Systems

sented in Section IV-A, was conducted to compare the different cold-start LPF models, including the proposed LPF-NIC model, several state-of-the-art LPF models and the DC PF model. The second experiment, which is presented in Section IV-B, was conducted to compare the proposed LPF-IC with another warm-start LPF model developed in [13]. Section IV-C studies the influence of the initial points on the performance of the warm-start LPF-IC method. The effect of approximation using nonlinear transformation is numerically investigated in Section IV-D.

A total of 25 benchmark power systems are employed as test examples, the sizes of which range from 24 to 9,241 buses with different loading conditions. The configurations of the test systems are summarized in Table I, where columns 3 through 8 indicate the number of corresponding elements. All of the test data can be accessed online in the package of MATPOWER without any modification [18]. All simulations are programed using MATLAB R2013a.

TABLE I
CONFIGURATION OF THE TEST SYSTEMS

No.	Name	Bus	Gen.	Branch	Tap	Phase Shifter
1	IEEE RTS	24	33	33	4	0
2	IEEE 30-Bus	30	6	41	0	0
3	IEEE 57-Bus	57	7	80	15	0
4	IEEE 118-Bus	118	54	186	9	0
5	IEEE 145-Bus	145	50	453	52	0
6	IEEE 300-Bus	300	69	411	62	0
7	PEGASE 1354	1354	260	1991	234	6
8	French 1888	1888	290	2531	405	4
9	French 1951	1951	366	2596	486	4
10	Polish 2383wp	2383	327	2896	170	6
11	Polish 2736sp	2736	270	3269	167	2
12	Polish 2737sop	2737	219	3269	168	2
13	Polish 2746wop	2746	431	3307	170	1
14	Polish 2746wp	2746	456	3279	169	1
15	French 2848rte	2848	511	3776	558	6
16	French 2868rte	2868	561	3808	606	6
17	PEGASE 2869	2869	510	4582	496	12
18	Polish 3012wp	3012	385	3572	201	0
19	Polish 3120sp	3120	298	3693	206	0
20	Polish 3375wp	3375	479	4161	383	2
21	French 6468rte	6468	399	9000	1319	19
22	French 6470rte	6470	761	9005	1333	16
23	French 6495rte	6495	680	9019	1359	17
24	French 6515rte	6515	684	9037	1367	16
25	PEGASE 9241	9241	1445	16049	1319	66

A. Comparison of the Cold-Start LPF Models

The LPF-NIC model (M0) is compared with several state-of-the-art cold-start LPF models, including the DC PF (DC) and those in [8] (S1), [11] (S2), and [12] (S3). Because the DC PF provides only an approximation of the active power, it is compared with the other models only in terms of the active branch flows. Although the reactive branch flow is not explicitly formulated in either [8] or [11], it can still be derived based on the concepts in these references as follows:

$$\text{S1:} \quad Q_{ij} \approx -\frac{b_{ij}}{2}(\delta_i V_i^2 - \delta_j V_j^2)^2 - \frac{g_{ij}}{t_{ij}}(\delta_i V_i^2 - \delta_j V_j^2), \tag{59}$$

$$\text{S2:} \quad Q_{ij} \approx -\frac{b_{ij}}{t_{ij}}\left(\frac{V_i}{t_{ij}} - V_j\right) - \frac{g_{ij}}{t_{ij}}(\theta_{ij} - \delta_{ij}). \tag{60}$$

As for the model in [12], we neglect its nonlinear loss component and employ only its linear part to perform a fair comparison with the other linear models. The AC PFs are also solved by the Newton-Raphson method with flat starts to yield benchmarked solutions. As indices for evaluation, the root-mean-squared (RMS) errors of a solution $\boldsymbol{x}$ with respect to the benchmarked solution $\boldsymbol{x}^*$ are defined as follows:

$$\Delta \boldsymbol{x}^{\text{RMS}} = \sqrt{\sum_{i=1}^{n}(x_i - x_i^*)^2 / n}. \tag{61}$$

1) Voltage magnitudes. Fig. 2 presents the RMS errors of voltage magnitudes of different LPF models. The errors of S1 are larger than those obtained using M0 in most cases. S2 has a similar performance to M0 and provides errors slightly larger than those obtained using M0. S3 yields larger errors than M0 in a number of test systems, including the 3rd, the 7th, the 8th, and the 20th through the 24th. Hence, M0 provides more accurate voltage magnitudes than the other three models.

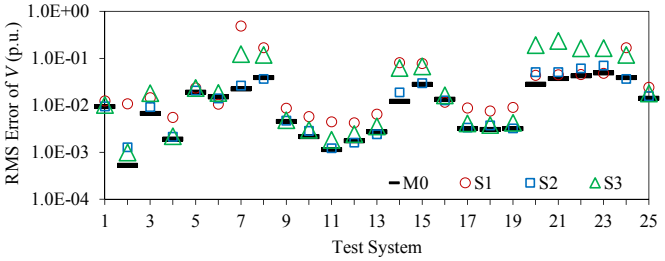

Fig. 2. Voltage magnitude errors of the different cold-start LPF models.

2) Branch flows. Fig. 3 displays the RMS errors of the active flows obtained using M0, S1, S2, S3, and DC. The errors of S1 and S3 are higher than those obtained using M0. The errors obtained using the S2 are typically larger than those of M0, although S2 performs better than S1. The DC PF provides comparable RMS errors to M0 in most cases for the active branch flows. Overall, M0 outperforms the other LPF models in approximating the active branch flows.

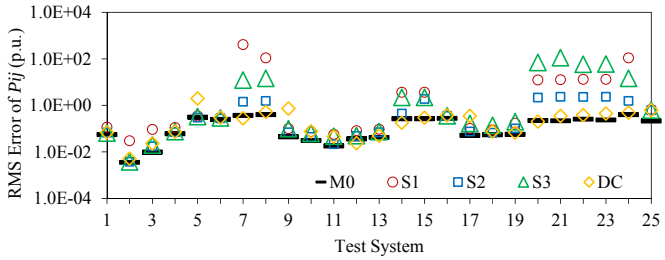

Fig. 3. Active branch flow errors of the different cold-start LPF models.

Fig. 4 shows the reactive branch flow errors of the different LPF models. The RMS errors of M0 are smaller than those of the other models. Similar observations can be made for the complex branch flow errors in Fig. 5. The comparative results suggest that M0 outperforms S1, S2, and S3 in approximating the reactive and complex branch flows.

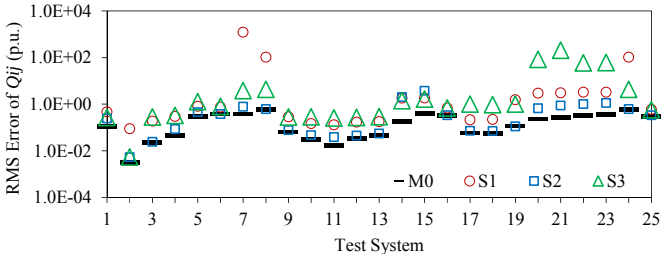

Fig. 4. Reactive branch flow errors of the different cold-start LPF models.

This article has been accepted for publication in a future issue of this journal, but has not been fully edited. Content may change prior to final publication. Citation information: DOI 10.1109/TPWRS.2017.2776253, IEEE Transactions on Power Systems

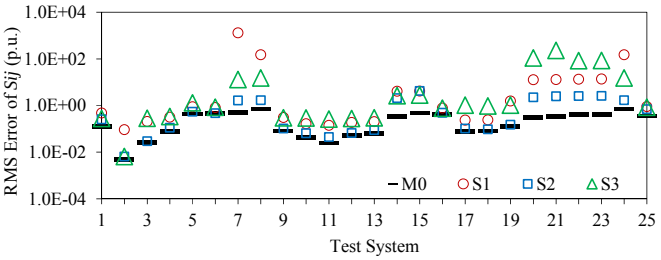

Fig. 5. Complex branch flow errors of different cold-start LPF models.

3) Active power losses. Fig. 6 exhibits the RMS errors of the branch active power loss given by M0, S1, and S3. Because the models of S2 and DC are assumed to be lossless, they do not yield any power losses. M0 yields the smallest active power loss errors in all test cases, whereas the errors of S1 and S3 are at least one order of magnitude larger than those of M0. This result indicates that M0 leads to more accurate active power losses than the other two models.

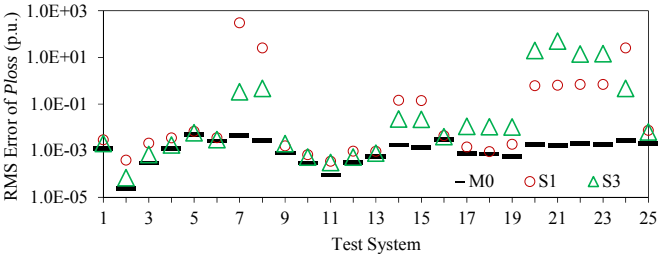

Fig. 6. Active power loss errors of the different cold-start LPF models.

4) Solution time. The computation time of solving the different PF models, including the AC PF (AC), is presented in Fig. 7. Significantly more time is needed to solve the AC PF than the other LPF models because solving the AC PF numerically requires an iterative procedure, whereas each of the LPF models, which are essentially linear equations, can be solved in one shot. The differences in the solution times required by the different LPF models are small, indicating that the computational efficiencies of the LPF models are similar. When M0 provides more accurate PF results than the other LPF models, its computational performance is still as good as the other LPF models.

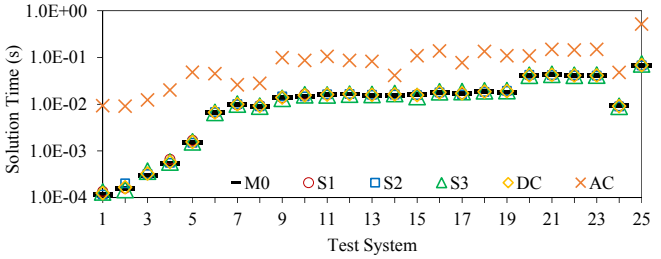

Fig. 7. Solution time consumed by solving the different cold-start PF models.

B. Comparison of the Warm-Start LPF Models

The warm-start LPF-IC (M1) is compared with the linearized PF model in [13] (S4) by solving the PFs in different test systems. The solutions of the DC PFs with flat voltage profiles are employed as initial points for inducing the linearized models of M1 and S4. Fig. 8 through Fig. 12 present the RMS errors of the voltage magnitudes, active branch flows, reactive branch flows, complex branch flows, and active power losses obtained by M1 and S4. Although S4 provides comparable results with M1 in several cases, it fails to produce reasonable results in some other cases, such as for test systems 20 through 24, for which the errors of S4 could be one order of magnitude larger than those of M1. For the active power losses, M1 also results in apparently smaller errors than S4. On the whole, M1 provides more accurate approximate PF solutions than S4.

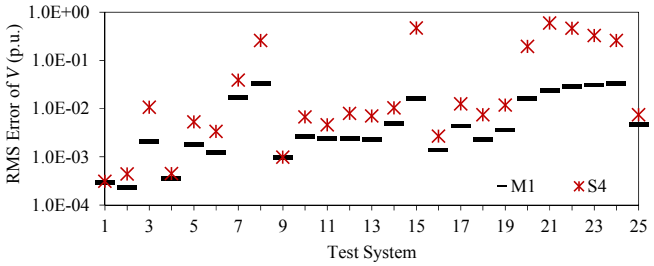

Fig. 8. Voltage magnitude errors of the different warm-start LPF models.

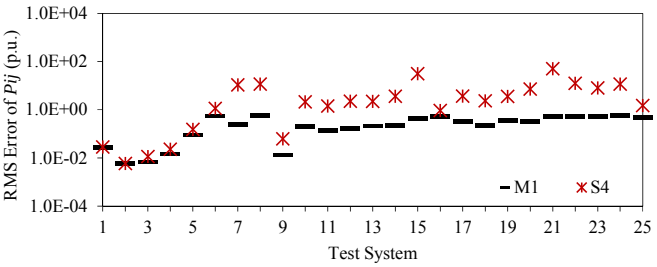

Fig. 9. Active branch flow errors of the different warm-start LPF models.

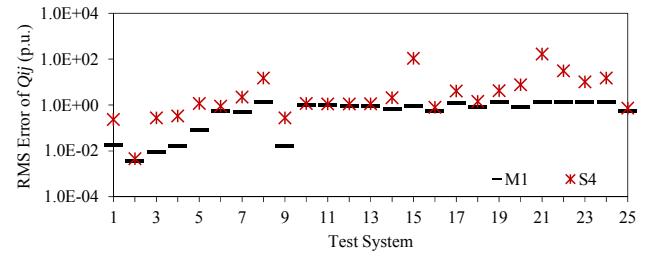

Fig. 10. Reactive branch flow errors of the different warm-start LPF models.

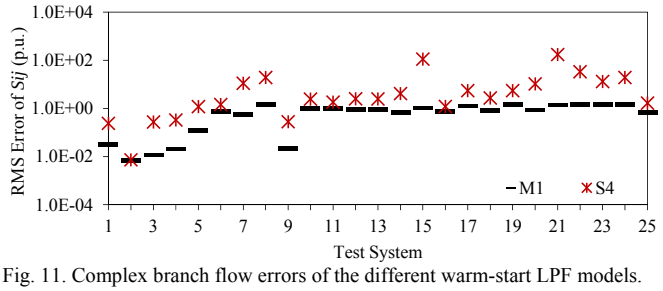

Fig. 11. Complex branch flow errors of the different warm-start LPF models.

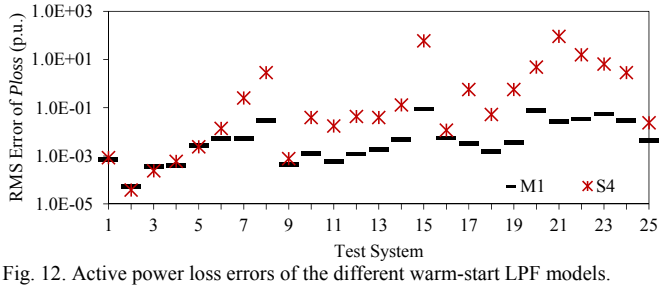

Fig. 12. Active power loss errors of the different warm-start LPF models.

C. Impact of the Compensation Points on the Performance of M1

The performance of M1 with different compensation points $\boldsymbol{x}^{(0)}$ was also investigated. Candidate $\boldsymbol{x}^{(0)}$ includes the following: (i) the flat start point with flat voltage profiles and zero phase angles, (ii) the solution to DC PF with flat voltage pro-

This article has been accepted for publication in a future issue of this journal, but has not been fully edited. Content may change prior to final publication. Citation information: DOI 10.1109/TPWRS.2017.2776253, IEEE Transactions on Power Systems

files, and (iii) the solution to M0. Each of these points is employed to calculate $\Delta \boldsymbol{d}(\boldsymbol{x}^{(0)})$ in (58), which is incorporated into the LPF-IC model. The LPF-ICs with these compensation points are denoted by M1-flat, M1-DC, and M1-M0, respectively. These models are tested using all of the aforementioned test systems.

Fig. 13 and Fig. 14 present the RMS errors of the voltage magnitudes and complex branch flows, respectively, obtained using different models, and the results from the cold-start M0 are also plotted as a reference. The errors of M1-flat are rarely larger than those of M0 in the test cases. The flat start is only a rough approximation of the exact solution of the PF, and the gaps between them are typically large. Hence, a flat start could result in a misleading IC the LPF model and thus deteriorate the accuracy of the approximation. This conclusion is consistent with the observation that the errors of M1-flat are larger than those of M0, as shown in Fig. 13 and Fig. 14.

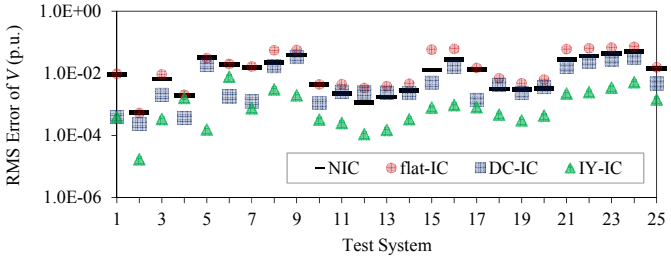

Fig. 13. Voltage magnitude errors obtained using the LPF-IC with different compensation points.

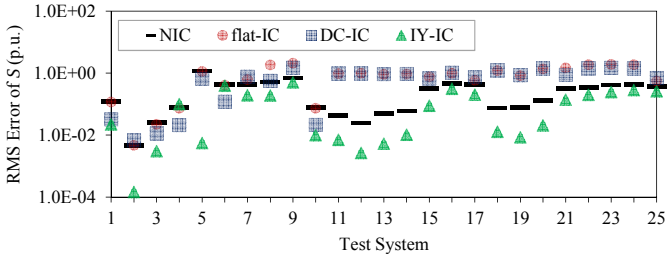

Fig. 14. Complex branch flow errors obtained using the LPF-IC with different compensation points.

The M1-DC outperforms the M1-flat in terms of the errors in both the voltage magnitudes and branch flows. This result is reasonable because DC PF generally provides more accurate approximations than the flat start in terms of the active power conditions. As shown in the figures, the M1-DC improves the accuracy of the voltage magnitudes slightly in certain cases. In contrast, because a DC PF solution still provides a trivial approximation to the voltage profiles, it could impair the quality of the solution when incorporated into the IC, as shown by the branch flow errors in Fig. 14.

As shown in Fig. 13 and Fig. 14, the errors are reduced significantly by the M1-M0 in most cases, indicating that the M1-M0 improves the accuracy of both the voltage magnitudes and branch flows in all test systems. This higher accuracy is achieved because M0, even without the IC, is able to yield an approximate PF solution that is close to the exact PF solution, as discussed in Section IV-A. Furthermore, solving M0 requires only a set of linear equations to be solved, and it is as easy as solving the DC PF, as shown in Fig. 7. Therefore, it is computationally trivial to use the solution of M0 to calculate the IC.

In summary, the compensation point must be selected carefully because it affects the solution quality of the LPF-IC. The solution to the LPF-NIC is typically a good choice that can potentially improve the accuracy in a warm-start LPF model.

D. Effect of Approximation Using Nonlinear Transformation

The AC PF model can be written in the following form:

$$\begin{aligned} P_i &= g_{ii}V_i^2 - \sum_{j\neq i}\left[g_{ij}(V_i^2 - V_iV_j\cos\theta_{ij}) + b_{ij}V_iV_j\sin\theta_{ij} \right] \\ Q_i &= -b_{ii}V_i^2 + \sum_{j\neq i}\left[b_{ij}(V_i^2 - V_iV_j\cos\theta_{ij}) - g_{ij}V_iV_j\sin\theta_{ij} \right] \end{aligned}. \quad (62)$$

V_i^2, $l_0^{\mathrm{V}} = V_i^2 - V_iV_j\cos\theta_{ij}$ and $l_0^{\theta} = V_iV_j\sin\theta_{ij}$ are the nonlinear terms in the AC PF equations presented in (62). To study the effect of nonlinear transformation, it is helpful to investigate the accuracy of approximating these nonlinear terms.

Except for the LTVM presented in this paper, other nonlinear transformation methods have also been applied to handle state variables and to approximate nonlinear terms. Table II summarizes the transformed state variables and approximations of nonlinear terms in AC PF using S1, S3 and the proposed method, respectively. In the proposed method, the nonlinear terms in P and Q equations are approximated in different forms, as indicated in the 3rd and 4th rows of Table II.

In this section, we compare the proposed method with other state-of-the-art nonlinear-transformation-based methods (S1 and S3) in terms of the accuracy of approximating these nonlinear terms. In real-life power networks, the shunt conductance (g_{ii}) and susceptance (b_{ii}) are typically small, so the influence of the term V_i^2 is negligible. We focus on the accuracy of approximating the other two terms.

TABLE II
NONLINEAR TRANSFORMATION AND APPROXIMATION OF LPF MODELS

Method	Independent variables		Nonlinear terms	
	Voltage	Angle	$l_0^{\mathrm{V}} = V_i^2 - V_iV_j\cos\theta_{ij}$	$l_0^{\theta} = V_iV_j\sin\theta_{ij}$
S1	V^2	$V^2\theta$	$\tilde{l}_{\mathrm{S1}}^{\mathrm{V}} = 0.95(V_i^2 - V_j^2)$	$l_{\mathrm{S1}}^{\theta} = 0.95(V_i^2\theta_i - V_j^2\theta_j)$
S3	$V^2/2$	θ	$\tilde{l}_{\mathrm{S3}}^{\mathrm{V}} = 0.5(V_i^2 - V_j^2)$	$\tilde{l}_{\mathrm{S3}}^{\theta} = \theta_{ij}$
M0 (for P)	$\ln(V)$	θ	$\tilde{l}_{\mathrm{P}}^{\mathrm{V}} = \dfrac{\ln(V_i) - \ln(V_j)}{1 - \ln(V_i)}$	$\tilde{l}_{\mathrm{P}}^{\theta} = \dfrac{\theta_{ij}}{1 - \ln(V_i)}$
M0 (for Q)	$\ln(V)$	θ	$\tilde{l}_{\mathrm{Q}}^{\mathrm{V}} = \dfrac{\ln(V_i) - \ln(V_j)}{1 - 2\ln(V_i)}$	$\tilde{l}_{\mathrm{Q}}^{\theta} = \dfrac{\theta_{ij}}{1 - 2\ln(V_i)}$

We define the following region of (V_i, V_j, θ_{ij}) that covers most of the normal operating states in practical power systems:

$$\Phi = \left\{ (V_i, V_j, \theta_{ij}) \middle| \begin{array}{l} 0.8 \le V_i \le 1.2,\ 0.8 \le V_j \le 1.2, \\ \left|V_i - V_j\right| \le 0.05, \left|\theta_{ij}\right| \le \pi/6 \end{array} \right\}, \quad (63)$$

over which the following RMS errors of approximation by each method are numerically calculated:

$$\varepsilon^{\alpha} = \sqrt{\frac{\int_{\Phi}\left[l_0^{\alpha}(V_i, V_j, \theta_{ij}) - \tilde{l}_{\beta}^{\alpha}(V_i, V_j, \theta_{ij}) \right]^2 \mathrm{d}V_i\mathrm{d}V_j\mathrm{d}\theta_{ij}}{\int_{\Phi}\mathrm{d}V_i\mathrm{d}V_j\mathrm{d}\theta_{ij}}}. \quad (64)$$

In (64), the superscript $\alpha \in$ {"V", "θ"} refers to either type of the nonlinear terms, and the subscript $\beta \in$ {"S1", "S3", "P", "Q"} represents the method for approximation. As shown in Table III, $\tilde{l}_{\mathrm{Q}}^{\mathrm{V}}$ and $\tilde{l}_{\mathrm{P}}^{\theta}$ provides the smallest RMS errors for l_0^{V}

This article has been accepted for publication in a future issue of this journal, but has not been fully edited. Content may change prior to final publication. Citation information: DOI 10.1109/TPWRS.2017.2776253, IEEE Transactions on Power Systems

and l_0^{θ}, respectively. This result reveals that the proposed method outperforms the others in approximating the nonlinear terms of AC PF within the predefined operating region.

TABLE III
RMS ERRORS OF APPROXIMATING NONLINEAR TERMS

Method		S1	S3	M0 (for P)	M0 (for Q)
Nonlinear terms	l_0^{V}	0.02639	0.00737	0.00766	**0.00681**
	l_0^{θ}	0.09428	0.02225	**0.01110**	0.11197

We note that for the same type of equation, the terms that approximate l_0^{θ} and l_0^{V} should have the same denominator in order to achieve linearizability of the equations. To make a tradeoff between the linearizability and approximation accuracy, we choose to use $\tilde{l}_P^{\theta}$ and $\tilde{l}_P^{V}$ to approximate l_0^{θ} and l_0^{V} in the P equations and $\tilde{l}_Q^{\theta}$ and $\tilde{l}_Q^{V}$ to approximate l_0^{θ} and l_0^{V} in the Q equations. As numerically shown above, although $\tilde{l}_Q^{\theta}$ and $\tilde{l}_P^{V}$ do not optimally approximate l_0^{θ} and l_0^{V}, they do not have significant impact on the approximation accuracy because the P and Q equations are mainly affected by the terms associated with l_0^{θ} and l_0^{V}, respectively, in strongly inductive power networks.

In summary, the overwhelming performance of the proposed model is attributed to the following two aspects. First, the nonlinear terms in the original AC PF equations are approximated more accurately using the proposed method than the other state-of-the-art methods. Second, in the proposed LPF model, different approximations are separately utilized in the P and Q equations, and they fit the dominating nonlinear terms in P and Q equations the best, separately.

V. CONCLUSIONS AND FUTURE WORK

This paper proposes an approximate LPF method that considers active and reactive power and transmission losses simultaneously. A general LPF model considering tap changers and phase shifters is derived using the LTVM. An approximation for branch power loss is developed, and approximate complex branch flows considering power loss are formulated. Two types of PF calculation methods are developed based on the proposed linear models, namely, cold-start without IC and warm-start with IC. Comparative simulations are conducted using a variety of large-scale test systems. The test results demonstrate that the proposed cold-start LPF-NIC and warm-start LPF-IC models approximate the PF solution more accurately than several state-of-the-art linear models in terms of the voltage magnitudes, branch load flows, and transmission power losses without additional computational burden. The compensation point does influence the solution quality of the LPF-IC significantly, and the proposed LPF-NIC can provide a proper compensation point to improve the accuracy of the LPF-IC. The overwhelming performance of the proposed model is due to its accurate approximation of nonlinear terms in AC PF equations.

The proposed LPF method could be applied in power system analysis and operation where PF modeling is needed. The proposed cold-start version model, i.e., the LPF-NIC, can be adopted in off-line applications where the base point of operation cannot be readily obtained, e.g., power system planning, day-ahead SCUC, CA, and reliability assessment. The proposed warm-start LPF-IC is particularly suitable for real-time analysis and decisions, e.g., look-ahead power dispatch, AVC, and online CA. When adopted to replace the nonlinear AC PF model, the proposed linear models could reduce the computational burden or the complexity of the optimization models. These issues could be further explored in future work.

REFERENCES

[1] A.J. Wood, B.F. Wollenberg, Power Generation, Operation and Control, 2nd Edition, John Wiley & Sons, New York, 1996.

[2] B. Stott, J. Jardim and O. Alsac, "DC Power Flow Revisited," *IEEE Trans. Power Syst.,* vol. 24, pp. 1290-1300, Aug. 2009.

[3] P. Sauer, "On the Formulation of Power Distribution Factors for Linear Load Flow Methods," *IEEE Trans. on Power Apparatus and Syst.,* vol. PAS-100, pp. 764-770, Feb. 1981.

[4] M. K. Enns, J. J. Quada, and B. Sackett, "Fast linear contingency analysis," *IEEE Trans. Power App. Syst.*, vol. PAS-101, no. 4, pp. 783-791, April 1982.

[5] M. Shahidehpour, H. Yamin, and Z. Li, *Market Operations in Electric Power Systems*. New York, NY, USA: Wiley, 2002.

[6] K. Purchala, L. Meeus, and R. Belmans, "Usefulness of DC power flow for active power flow analysis," in *Proc. IEEE PES General Meeting*, 2005, vol. 1

[7] H. Sun, Q. Guo, B. Zhang, W. Wu, and B. Wang, "An Adaptive Zone-Division-Based Automatic Voltage Control System With Applications in China," *IEEE Trans. Power Syst.,* vol. 28, pp. 1816-1828, May 2013.

[8] S. M. Fatemi, S. Abedi, G. B. Gharehpetian, S. H. Hosseinian, and M. Abedi, "Introducing a Novel DC Power Flow Method With Reactive Power Considerations," *IEEE Trans. Power Sys.,* vol. 30, pp. 3012-3023, Nov. 2015.

[9] S. Bolognani and S. Zampieri, "On the Existence and Linear Approximation of the Power Flow Solution in Power Distribution Networks," *IEEE Trans. Power Sys.,* vol. 31, pp. 163-172, Jan. 2016.

[10] H. Ahmadi, J. R. Marti and A. von Meier, "A Liner Power Flow Formulation for Three-Phase Distribution Systems," *IEEE Trans. Power Sys.,* vol. 31, pp. 5012-5021, Nov. 2016.

[11] J. Yang, N. Zhang, C. Kang, and Q. Xia, "A State-Independent Linear Power Flow Model with Accurate Estimation of Voltage Magnitude," *IEEE Trans. Power Sys.,* accepted.

[12] Z. Yang, H. Zhong, Q. Xia, and C. Kang, "A novel network model for optimal power flow with reactive power and network losses," *Electric Power Systems Research,* vol. 144, pp. 63-71, Mar. 2017.

[13] Z. Yang, H. Zhong, A. Bose, T. Zheng, Q. Xia, and C. Kang, "A linearized OPF model with reactive power and voltage magnitude: A pathway to improve the MW-Only DC OPF," *IEEE Trans. Power Syst.,* accepted.

[14] K. Dvijotham, E. Mallada and J. W. Simpson-Porco, "High-Voltage solution in radial power networks: Existence, properties, and equivalent algorithms," *IEEE Control Systems Letters,* vol. 1, no. 2, pp. 322-327, Oct. 2017.

[15] R. D. Zimmerman, C. E. Murillo-Sanchez and R. J. Thomas, "MATPOWER: Steady-State operations, planning, and analysis tools for power systems research and education," *IEEE Trans. Power Syst.,* vol. 26, pp. 12-19, Feb. 2011.

[16] S. Sivanagaraju and B. V. Rami, *Reddy: Electrical Power System Analysis*. NewDelhi, India: Laxmi, 1998, p. 88.

[17] H. Zhong, Q. Xia, Y. Wang, and C. Kang, "Dynamic economic dispatch considering transmission losses using quadratically constrained quadratic program method," *IEEE Trans. Power Syst.*, vol. 28, pp. 2232-2241, Aug. 2013.

[18] MATPOWER - A MATLAB Power System Simulation Package v6.0b2. [Online]. Available: http://www.pserc.cornell.edu/matpower/